High-severity wildfire leads to multi-decadal impacts on soil biogeochemistry in mixed-conifer forests

Nicholas C. Dove,[1,7] Hugh D. Safford,[2,3] Gabrielle N. Bohlman,[4] Becky L. Estes,[5] and Stephen C. Hart[6,8]

[1]*Environmental Systems Graduate Group, University of California, Merced, California 95343 USA*
[2]*Department of Evolution and Ecology, University of California, Davis, California 95616 USA*
[3]*USDA-Forest Service, Pacific Southwest Region, Vallejo, California 94592 USA*
[4]*USDA-Forest Service, 1711 South Main Street, Yreka, California 96097 USA*
[5]*USDA-Forest Service, Pacific Southwest Research Station, Redding, California 96002 USA*
[6]*Department of Life & Environmental Sciences and Sierra Nevada Research Institute, University of California, Merced, California 95343 USA*

Abstract. During the past century, systematic wildfire suppression has decreased fire frequency and increased fire severity in the western United States of America. While this has resulted in large ecological changes aboveground such as altered tree species composition and increased forest density, little is known about the long-term, belowground implications of altered, ecologically novel, fire regimes, especially on soil biological processes. To better understand the long-term implications of ecologically novel, high-severity fire, we used a 44-yr high-severity fire chronosequence in the Sierra Nevada where forests were historically adapted to frequent, low-severity fire, but were fire suppressed for at least 70 yr. High-severity fire in the Sierra Nevada resulted in a long-term (44 +yr) decrease (>50%, $P < 0.05$) in soil extracellular enzyme activities, basal microbial respiration (56–72%, $P < 0.05$), and organic carbon (>50%, $P < 0.05$) in the upper 5 cm compared to sites that had not been burned for at least 115 yr. However, nitrogen (N) processes were only affected in the most recent fire site (4 yr post-fire). Net nitrification increased by over 600% in the most recent fire site ($P < 0.001$), but returned to similar levels as the unburned control in the 13-yr site. Contrary to previous studies, we did not find a consistent effect of plant cover type on soil biogeochemical processes in mid-successional (10–50 yr) forest soils. Rather, the 44-yr reduction in soil organic carbon (C) quantity correlated positively with dampened C cycling processes. Our results show the drastic and long-term implication of ecologically novel, high-severity fire on soil biogeochemistry and underscore the need for long-term fire ecological experiments.

Key words: chronosequence; extracellular enzyme activity; fire suppression; microbial biomass; microbial ecology; microbial respiration; nitrogen cycle; Sierra Nevada; soil organic carbon.

Introduction

Wildfire has historically regulated carbon (C) and nitrogen (N) cycling in yellow pine and mixed-conifer forests of the Sierra Nevada and other fire-adapted ecosystems commonly found throughout the western United States of America (Johnson et al. 2008). However, due to the interaction between increasing forest fuels (due to long-term fire suppression and early forest management practices) and the rapidly warming climate, contemporary fires in these ecosystems are outside their natural range of variation and are currently burning at

higher severities than their pre-1850 counterparts (Miller et al. 2009*b*, Safford and Stevens 2017). This departure from historical conditions has the potential to affect the resistance and resilience of many soil processes to fire (Fig. 1). The importance of fire effects on forest soil biogeochemistry has gained attention in recent years (e.g., Nave et al. 2011, Caon et al. 2014, Butler et al. 2018, Pellegrini et al. 2018); however, much of this work has focused on disturbances within the range of natural variation for that ecosystem. For example, many have studied stand-replacing fire in boreal or subalpine forests (Smithwick et al. 2005, Turner et al. 2007, Holden et al. 2016) or low-severity, prescribed fire in seasonally dry, temperate forests (Kaye and Hart 1998, Kaye et al. 2005, Grady and Hart 2006, Fultz et al. 2016). There has been relatively less focus on how C and N cycling processes respond to and recover from ecologically novel
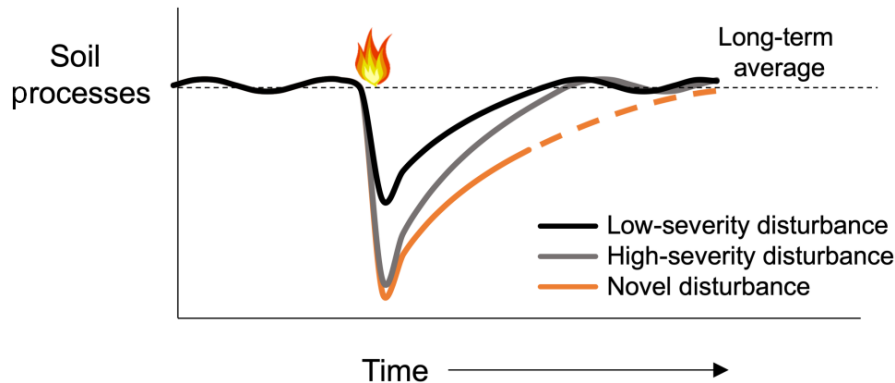
Fig. 1. Conceptual model of hypothesized recovery of ecosystem function after different disturbances. We hypothesize that, whereas high-severity disturbances (gray line) may result in greater functional responses than low-severity disturbances (black line), resilience is most impacted by novel disturbances (orange line; e.g., wildfire with severity greater than the historic range of variation). The orange line is dashed at the tail end of recovery to indicate that ecosystems may not recover to predisturbance conditions after novel disturbances.

fire (i.e., fire severity outside the natural range of variation).

Before major Euro-American settlement began in the mid-1800s, the fire regime of yellow pine and mixed-conifer (YPMC) forests in California and the southwestern United States was dominated by frequent fires (fire return interval of one to two decades) of low to moderate vegetation burn severity, and high mortality of canopy trees was relatively rare (Fry et al. 2014, Safford and Stevens 2017). Trend assessments carried out since 1984 (the beginning of the LANDSAT data set) show that the severity of wildfires in YPMC and similar forest types is increasing in California and the southwestern United States. Both the total area burned at high severity and the mean and maximum sizes of high-severity burn patches within fires are increasing (Miller et al. 2009b, Mallek et al. 2013, Dillon et al. 2016, Steel et al. 2018). Clearly, the modern fire regime is well outside the natural range of variation for fire severity, and the ecosystem-level effects of many modern fires can be reasonably characterized as "novel" (Miller and Safford 2017, Safford and Stevens 2017).

Direct and indirect impacts of fire on soil biogeochemistry and the relative magnitude of these effects vary with time since fire (Hart et al. 2005). On shorter time scales, wildfire has been shown to decrease soil extracellular enzyme activity (Boerner et al. 2008, Taş et al. 2014, Knelman et al. 2017) and microbial respiration (Grady and Hart 2006) due to the combustion of microbial biomass and soil organic C (SOC; Miesel et al. 2011, Knelman et al. 2015). Nitrogen availability within a few years after fire is generally high (Covington and Sackett 1992, DeLuca and Sala 2006), originating from fire-induced N mineralization (St. John and Rundel 1976), increased rates of organic matter decomposition (Kaye and Hart 1998), and increased N-fixing plant abundance (Johnson et al. 2005). Increases in N availability can result in lower N-limitation to soil microorganisms and increase

nitrification (Kurth et al. 2014, Hanan et al. 2016). In the longer term, however, as plants recolonize post-fire, they begin to exert a greater influence over soil microbial communities through root exudation, plant litter inputs, increased nutrient uptake, and formation of symbioses with soil microorganisms. Thus, in the longer term, plant communities have been suggested to be the primary drivers of soil biogeochemical processes (Hart et al. 2005).

Ecologically novel, high-severity fire likely exacerbates the response and lengthens the recovery of soil biogeochemical processes compared to historical fires. Global change (including changing fire regimes) alters the selective pressures that organisms have been evolutionarily adapted to. Thus, the microbial communities, which control C and N cycling in soils, could be maladapted to these ecologically novel disturbances and post-fire conditions. This could reduce the resiliency of ecological functions that these organisms provide, hampering the recovery of the ecosystem. For example, under simulated drought conditions, plants responded positively when grown with drought-adapted microbial communities (Lau and Lennon 2012), showing that the adaption (or maladaptation) of microbial communities to global change can have ecosystem-level implications. However, the impact of ecologically novel fire on soil microbial communities and their function has yet to be fully elucidated.

We evaluated the long-term (40+ yr) impact of ecologically novel, high-severity fire on soil C and N cycling using a wide array of biogeochemical assays and rate measurements using space for time substitution. We hypothesize that novel, high-severity fire will cause multi-decadal impacts on site and soil properties (e.g., vegetation, temperature and moisture dynamics, pH, SOC, nutrient availability, and microbial biomass), which will result in changes in the rates of biogeochemical processes. Specifically, we expect decreased soil extracellular enzyme activities and respiration and increased soil net

N mineralization, net nitrification, and nitrifier activity (assessed by nitrification potential and N_2O fluxes) following high-severity fire in YPMC ecosystems. In the short term (<10 yr), we hypothesize that impacts will be due to the *direct* impacts of fire: combustion of SOC and microbial biomass and mineralization of N. In the longer term (>10 yr), we hypothesize that impacts will be due to the indirect effect of fire on soils through vegetation (i.e., plant cover type would have a greater effect with increased time since fire). Finally, we hypothesize that these effects will be more pronounced when soils are wetter and microbial activity is higher. Our overall goal is to determine the long-term impact of novel, high-severity fire on soil biogeochemical processes in order to quantify the resilience and identify the drivers of these processes at different stages of recovery. Developing a mechanistic understanding of the effects of high-severity fire and time since fire on soil biogeochemistry is critical for predicting how ecosystems respond to (and subsequently recover from) fire disturbances with severities outside their range of historic variability. Such information will be useful in management of fire-suppressed temperate forests and mitigation against the effects of these exceptional disturbance events (Adams 2013, Stephens et al. 2014).

Methods

Site description and experimental design

The study was conducted on the Eldorado National Forest, which is located in the Central Sierra Nevada of California, an area historically fire suppressed like much of western North America (Fig. 2, Safford and van de Water 2014). We sampled in areas of varying time since stand-replacing wildfire using a fire chronosequence in South Fork of the American River watershed. The fire sites are the King Fire (4 yr post-fire, 48% of fire area burned at high vegetation burn severity), the Freds Fire (13 yr post-fire, 58% high severity), the Cleveland Fire (25 yr post-fire, 64% high severity), and the Pilliken Fire (44 yr post-fire, >50% high severity; Bohlman et al. 2016). The spatial extent of high-severity burning in these fires is far outside the natural range of variation, which ranged from about 5% to 15% of the area of the average fire before Euro-American settlement of the region (Safford and Stevens 2017). We incorporated sites throughout the study area that had not burned since at least 1908 (Safford and van de Water 2014), which is the maximum period for which we know that no recorded burning occurred. We operationally defined this as our late successional site (>115 yr post-fire).

A fire chronosequence relies on the assumption that the variation in space (among sites) is equal to the variation in time since fire (Pickett 1989). This technique has been increasingly employed as a method for understanding the long-term trajectories of ecosystems post-fire (Kurth et al. 2013, Fest et al. 2015, Bohlman et al. 2016,

Holden et al. 2016, Sun et al. 2016). Although chronosequences may not always be ideal for measuring temporal effects due to inherent differences in site properties and life histories, we minimized these limitations through careful plot selection. Late successional (i.e., pre-fire) vegetation at all sites is characterized as mixed conifer forest. Dominant species include ponderosa pine (*Pinus ponderosa*), Jeffrey pine (*P. jeffreyi*), Douglas-fir (*Pseudotsuga menziesii*), white fir (*Abies concolor*), incense-cedar (*Calocedrus decurrens*), black oak (*Quercus kellogii*), and canyon live oak (*Q. chrysolepis*). Prior to fire, the 4-, 13-, 25-, and >115-yr sites had similar normalized difference vegetation index values (repeated-measures ANOVA, $P = 0.178$; data from Robinson et al. 2017), which correlates with the photosynthetic capacity of vegetation (the 44-yr site burned before the data record of 1984). Soils are in the suborder Xerepts, with either an umbric or ochric epipedon (USDA-NRCS 2015). Furthermore, all plots have a southern aspect (90°270°), are on moderate slopes (10%–20%, characteristic of the fire affected areas), and are between 1,100–1,300 m elevation.

Because we were interested in the unassisted recovery after high-severity fire, we sampled only in areas that were not managed post-fire (e.g., salvage logging, herbicide application, planting) and were classified as high-severity burns (>75% basal area mortality of dominant and codominant canopy trees). All areas were salvage logged in the 44-yr site, but the plots selected at this site were not manipulated further. While salvage logging may affect nutrient budgets and hydrologic regimes critical in early stand development (Johnson et al. 2005, Jennings et al. 2012), McGinnis et al. (2010) found no difference in shrub or grass cover between salvage logged and control sites in the Sierra Nevada. It is reasonable to conclude that salvage logging only minimally affected microbial communities and their processes at this site because long-term impacts of fire on microbial communities are hypothesized to be mainly influenced by live aboveground vegetation (Hart et al. 2005). Burn severity was assessed using delta normalized burn ratio (dNBR; Miller and Thode 2007) on Landsat imagery for the three most recent fires; for the 44-yr site, dNBR was determined using a 1974 false-color composite Landsat Multispectral Scanner System (MSS) image because this fire occurred before Landsat was launched (Bohlman et al. 2016). Vegetation burn severity (as used in our study) does not always correlate well with soil burn severity (Safford et al. 2008, Miesel et al. 2018). However, comparisons among fires in different years are difficult due to changing methods in soil burn severity mapping. The California vegetation burn severity classification we used is standardized and objectively determined based on published relationships between the Landsat data and field conditions (e.g., Miller and Thode 2007, Miller et al. 2009a, b). We were more comfortable using these more standardized products to map fire severity in our four chronologically disparate fires
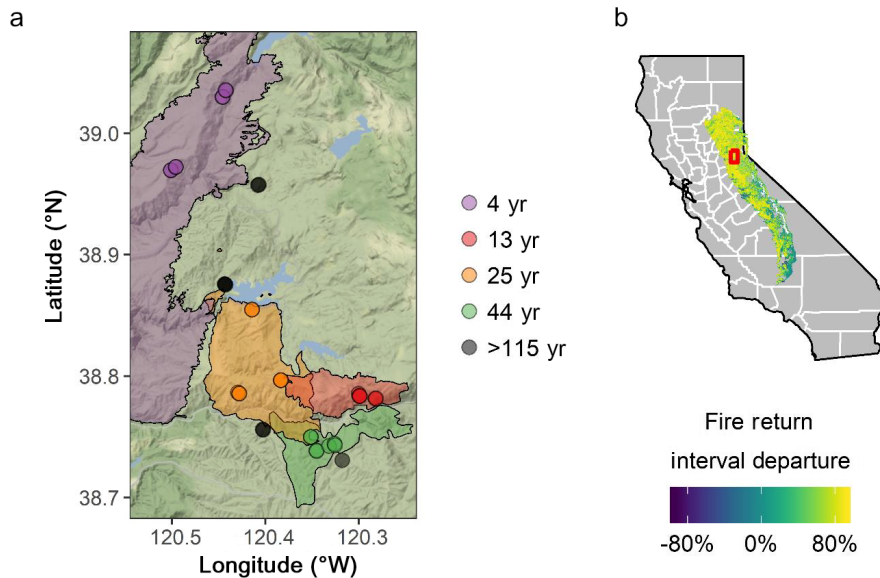
FIG. 2. Map of the Central Sierra Nevada Fire Chronosequence. (a) Symbols denote approximate locations of plots and polygons show fire perimeters (plots are at least 150 m apart and may not be visibly distinguishable at the spatial scale). (b) Fire return interval departure (Safford and van de Water 2014) is plotted for the Sierra Nevada with a red rectangle denoting the extent of the chronosequence area. Higher values represent greater fire suppression, and white lines show county boundaries for reference.

than the much more idiosyncratic soil burn severity maps (Safford et al. 2008).

Each site consisted of six to eight plots separated by at least 150 m (the 13 yr and 44 yr sites had only six and seven plots, respectively, due to sampling area constraints; all other sites had eight plots). Plot-centers were chosen randomly a priori using a GIS layer of appropriate site polygons (i.e., similar soils, elevation, aspect, burn severity, and management). Each plot was defined by a 5 m radius from plot center. Within each plot, we sampled one point under each of the available lowest stratum cover types. Cover types were tree (e.g., *Abies concolor*, *Pinus ponderosa*, *Quercus* spp.), seedling (e.g., *Pinus ponderosa*), shrub (*Arctostaphylos* spp., *Salix* spp.), nitrogen-fixing plant (*Ceonothus* spp., *Chamaebatia foliolosa*), herbaceous (e.g., *Carex* spp., Poaceae), and bare soil. When multiple representatives of the same cover type occurred within a plot (which occurred frequently), we sampled under the representative closest to plot center.

Soil sampling and preparation

We sampled mineral soil at two periods during 2017 (8–15 June and 6–14 September), representing two extremes of seasonal soil moisture and microbial activity in the Sierra Nevada (Hart et al. 1992, Qi and Xu 2001). The organic horizon was removed with a sterile, gloved hand, and a 2 cm diameter soil corer sterilized with 10% bleach followed by 70% ethanol was used to sample the top 5 cm of mineral soil at each point. We did not sample the organic horizon, because many of the 4- and 13-yr plots did not have one, and we decided to keep the sampling among sites consistent. To collect enough soil from each point (~100 g), we took and composited multiple (~10) cores within a 20-cm diameter area within a given cover-type stratum. Soil samples were placed in a sterile bag and immediately placed on blue ice (4°C). Upon returning to the laboratory, soils were sieved field-moist (<2 mm; sieve sterilized with 70% ethanol before and between samples) and were subsampled to be frozen (−20°C), refrigerated (4°C), or air dried until further analysis.

Site physical, chemical, and vegetative properties

Hobo Onset temperature sensors (UA-002-08; Bourne, Massachusetts, USA) were deployed at the center of each plot buried to a depth of 5 cm into the mineral soil. They recorded temperature every 2 h from 3 December 2016, until 15 May 2018, to determine potential differences in the soil thermal environment among cover-type strata and sites.

In addition to measuring gravimetric water content at each sample time, we measured the water holding capacity (WHC) of the soils during the June sampling event to understand the longer-term soil moisture dynamics in the field. Briefly, 10 g of field-moist soil was saturated with 50 g of deionized water and drained for 24 h using a funnel with Whatman 42 filter paper (>2.5 μm retentiveness) into a 1-L screw-top jar. Soils were loosely covered with the lid of the Mason jar to minimize evaporation. Water drained by gravity was weighed and WHC was calculated as the sum of the undrained water and field-moist gravimetric water content of the soil.

Prior to C and N analysis, air-dried soils from the June sampling event were ground to a fine powder using mortar and pestle. Approximately 10 mg of oven-dry, ground soil was weighed into tin capsules, and these samples were analyzed for total C and N by continuous-flow, direct combustion and mass spectrometry using the ECS 4010 CHNSO analyzer (Costech Analytical Technologies, Valencia, California, USA). Air-dried soils from the June sampling event were analyzed for pH in a 1:2 w/v ratio of soil to both deionized water and 0.01 mol/L $CaCl_2$ solutions with an Orion DUAL STAR pH meter (Thermo Fisher Scientific, Waltham, Massachusetts, USA).

We measured available inorganic N and P using ion-exchange resin bags. Bags were buried at 5-cm depth in the mineral soil at each sampling point and deployed during two time periods: 17–26 October 2016 until 8–15 June 2017 and 8–15 June 2017 until 6–14 September 2017, which were operationally defined as "wet" and "dry" seasons, respectively. We extracted ion-exchange resin with 2 mol/L KCl following Binkley and Matson (1983), and extracts were analyzed for ammonium, nitrate, and orthophosphate colormetrically using the Lachat AE Flow Injection Auto analyzer (Lachat Instruments, Milwaukee, Wisconsin, USA). Final concentrations were normalized by oven-dry resin mass and length of field incubation.

We used the line–point intercept method to estimate relative proportions of cover type within each plot (Parker 1951). We set up a 10-m transect, which was bisected by the plot center. A random bearing was selected to determine the orientation of each transect. Starting at 1 m, we recorded the substratum cover type (i.e., tree, seedling, shrub, nitrogen-fixing plant, herbaceous, bare) along the transect at 1-m increments for nine total measurements per plot, which we translated into percent cover.

Microbial biomass

We measured microbial biomass C and N for the June samples by chloroform fumigation-extraction (Vance et al. 1987, Hart and Firestone 1991, Haubensak et al. 2002). Briefly, 20 g of previously frozen and thawed, field-moist mineral soil was split into two equal samples. The non-fumigated sample was immediately extracted with 0.5 mol/L K_2SO_4, and the fumigated sample was incubated for seven days in a chloroform-filled desiccator. After fumigation, the fumigant was removed using repeated evacuations and the samples were then extracted with 0.5 M K_2SO_4. Fumigated and non-fumigated extracts were analyzed on a total organic C and total N analyzer (Shimadzu TOC-Vcsh with TNM-1 Total Nitrogen Measuring Unit, Kyoto, Japan). The difference in C and N concentration between these extracts is the chloroform-labile C and N pools, respectively. We used an extraction efficiency factor (k_{eC}) of 0.45 to convert chloroform-labile C to microbial C (Beck et al.

1997) and an extraction efficiency factor (k_{eN}) of 0.54 to convert chloroform-labile N to microbial N (Brookes et al. 1985). The mass ratio of microbial C:N was calculated to evaluate changes in microbial biomass stoichiometry. Performing chloroform fumigation-extraction on frozen soils may slightly affect the absolute values, but the relatively differences among treatments are generally unaffected (Hart and Firestone 1991, Stenberg et al. 1998).

Extracellular enzyme assays

We measured potential extracellular enzyme activity of β-glucosidase (BG), N-acetylglucosaminidase (NAG), and acid phosphatase (AP) fluorometrically following Bell et al. (2013). Briefly, an 800-μL soil slurry consisting of 2.75 g of field-moist soil in 91 mL of 50 mmol/L sodium acetate buffer (pH = 5.5) was incubated with 200 μL of each of the 100 μmol/L 4-methylumbelliferone (MUB)-linked substrates. After a 3-h incubation at 20°C, plates were centrifuged and supernatant was transferred to a black, flat-well plates. Fluorescence was measured on a Tecan M200 Pro (Tecan Group, Männedorf, Switzerland) using an excitation wavelength of 365 nm and an emission wavelength of 450 nm. We used the same substrate concentration and incubation time as Bell et al. (2013) instead of optimizing these assay parameters for our soils. Hence, our enzyme activities may be underestimated for some plots; however, we were still able to observe significant differences in enzyme activities along the chronosequence. Similarly to Bell et al. (2013), we did not include analytical replicates because we chose to maximize field replication.

The enzyme BG catalyzes the hydrolysis of ether bonds in polysaccharides releasing glucose, and is thus involved in the degradation of organic C. The enzyme NAG is involved in releasing N-acetylglucosamine from oligosaccharides such as chitin and peptidoglycan, and thus is considered an N-acquiring enzyme. The enzyme AP is involved in releasing phosphate from ester bonds, representing a P-mineralizing enzyme (Burns et al. 2013). Extracellular enzyme activities were expressed on oven-dry soil mass, SOC concentration, and microbial biomass C bases. The first two bases reflect ecosystem-level properties, while the third represents a microbial community-level property. Expressing activity on a microbial biomass basis represents the nutritional status of the microbial community, which allows comparisons across vastly different ecosystems (Boerner et al. 2005).

Microbial activity and net N mineralization

We measured heterotrophic, methane-oxidizer, and nitrifier microbial activity by carbon dioxide (CO_2), methane (CH_4), and nitrous oxide (N_2O) efflux, respectively, without substrate additions ex situ following Zibilske (1994). Briefly, 20 g of refrigerated, field-moist soils were adjusted to WHC and incubated in the dark

for 31 d at 21.5°C ($\pm$1°C) in 1-L Mason jars fitted with rubber septa. We sampled 16 mL of the headspace at day 3, 9, 17, and 31. After each sampling date, jars were opened and flushed with ambient air. Headspace samples were then analyzed for CO_2, CH_4, and N_2O by gas chromatography using Shimadzu GC-2014 fitted with thermal conductivity, flame ionization, and electron capture detectors (Shimadzu Corporation, Columbia, Maryland, USA). Specific rates of net C mineralization were calculated by dividing the rates of CO_2–C efflux over the 31-d period by the soil total C concentrations.

Inorganic N pool sizes before and after the 31-d incubation were determined by extracting 10 g (WHC mass) subsamples with 50 mL of 2 mol/L KCl, and analyzing the filtered extracts for NH_4^+ and NO_3^- as described previously. Net N transformation rates were determined by the net changes in inorganic N pools over the 31-d incubation period (Binkley and Hart 1989).

Nitrification potential

We estimated potential rates of nitrification using the shaken soil-slurry method (Hart et al. 1994), which approximates the capacity of ammonia oxidation in soil. Briefly, we created a soil slurry of 15 g of field-moist soil in a 100 mL NH_4^+ and PO_4^{3-} solution (1.5 mmol/L of NH_4^+ and 1 mmol/L of PO_4^{3-}) in a 250-mL flask and capped with a rubber stopper. The high concentrations of NH_4^+ and PO_4^{3-} ensure that nitrification is not substrate limited. Flasks were shaken (180 rpm) for 24 h. At 2, 4, 22, and 24 h, 10 mL of suspension was removed from each flask and centrifuged at 8000 $\times$g for 8 min. The supernatant (5 mL) was removed from the centrifuged soil slurry, placed into a disposable polypropylene tube, capped, and stored at -20°C until analysis for NO_3^- as described above. Nitrification potential is calculated as the rate of NO_3^- accumulation over time.

Statistical analyses

All statistical analyses were conducted in R (R Development Core Team 2008) using the car (Fox and Weisberg 2011), lme4 (Bates et al. 2015), and MuMIn (Barton 2018) packages. Significance was determined at the $\alpha = 0.05$ level for all statistical tests. Marginal statistical significance was determined at the $\alpha = 0.10$ level. The replicated regression experimental design (Cottingham et al. 2005) allowed us to analyze our chronosequence using both regression and analysis of variance (ANOVA). Hence, we were able to robustly determine biogeochemical relationships with time since fire using regression, while also allowing for ANOVA and Tukey's test of honestly significant differences to determine differences among sites.

We assessed the recovery of biogeochemical properties and processes at the plot scale. At the plot scale, data were proportionally averaged by the relative abundance of cover types for each plot. These data were then analyzed using mixed-effects models and mixed-design ANOVAs with time since fire and sample date as fixed factors, and plot as a random factor. We assessed the importance of cover type in controlling soil biogeochemical processes (e.g., extracellular enzyme activity, microbial activity, and N transformations) at the sample scale and during the June sampling date when the soils were wettest and the greatest differences among sites and cover types were expected. At the sample scale, data were analyzed using ANOVA with fire site, substratum cover type, and their interaction as independent variables. We assessed differences in vegetative cover-type compositions using a chi-squared independence test.

For all statistical analyses, we used QQ plots and scale-location plots to inspect normality and homoscedasticity, respectively. If these assumptions were not met, data were natural-log-transformed, verified for normality and homoscedasticity, and reanalyzed (as was the case for inorganic N assessed by resin bags, CH_4 and N_2O effluxes, extracellular enzyme activities, and N transformation processes including nitrification potential).

Results

Site and soil characteristics

Cover-type composition changed significantly among chronosequence sites (χ^2, $P < 0.001$, Fig. 3). Between the most recent fire site (4 yr) and latest successional site (>115 yr post-fire), tree cover increased from 8.3% to 77.8%, while N-fixing plant cover decreased from 65.3% to 4.2%. Grass and shrub (non-N-fixing) cover was highest in the 25- and 44-yr fire sites, reaching maxima of 33.3% for both.

Soil characteristics (e.g., soil total C and N, WHC, resin-available N and P, and microbial biomass C and N) did not differ by or interact with cover type ($P > 0.100$; data not shown), but at the plot scale, soil physical and chemical characteristics were significantly affected by time since fire (Table 1). Total C and N in the upper 5 cm of the mineral soil increased with time since fire (soil C, $P < 0.001$, $R^2 = 0.33$, $n = 37$, Fig. 4a; soil N, $P = 0.014$, $R^2 = 0.14$, $n = 37$), and the values of these soil characteristics in the 4- through 44-yr post-fire sites were about 50% of the values in the >115-yr site (Table 1). During the wet season (November-June), inorganic N availability assessed by ion-exchange resin was elevated in the 4-yr site (Table 1); NO_3^- availability was on average 73 times that of the other sites ($P < 0.001$), and NH_4^+ availability was over six times greater in the 4-yr site than the 44-yr site ($P = 0.015$), although statistically similar to the other sites. During the dry season (June-September), only the NH_4^+ availability differed by site ($P = 0.014$), with the 4- and 13-yr sites 2.8 and 4.7 times higher than the >115-yr site, respectively (4 yr, $P = 0.033$; 13 yr, $P = 0.014$). During the wet season, the PO_4^{3-} availability was four orders of magnitude higher in
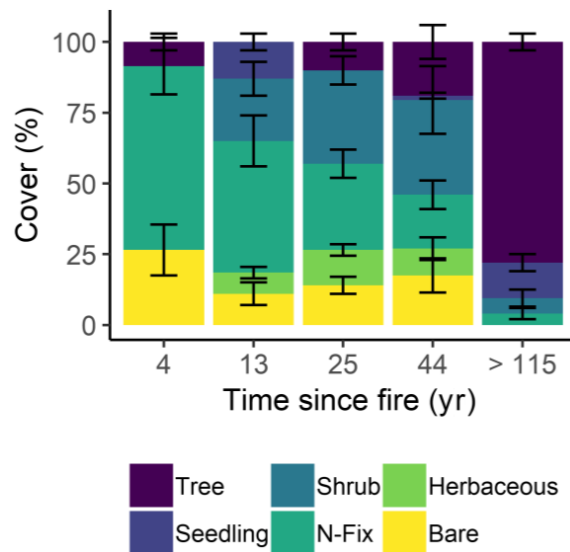
FIG. 3. Plot-scale mean percent plant cover types for each chronosequence site ($n = 8$). Cover types are tree (e.g., *Abies concolor*, *Pinus ponderosa*, *Quercus* spp.,), tree seedling (e.g., *Pinus ponderosa*), shrub (*Arctostaphylos* spp., *Salix* spp.), nitrogen-fixing plant (N-Fix; *Ceanothus* spp., *Chamaebatia foliolosa*), herbaceous (e.g., *Carex* spp., Poaceae), and bare soil. Error bars show the standard error of the mean (13-yr site, $n = 6$; 44-yr site, $n = 7$; all other sites, $n = 8$).

the >115-yr site compared to the 4-yr site ($P = 0.001$), and increased logarithmically with time since fire ($P < 0.001$, $R^2 = 0.53$, $n = 15$, Table 1). The availability of PO_4^{3-} was not significantly different between the 13-yr site and the >115-yr sites. During the dry season, the relationship between time since fire and PO_4^{3-} availability was not significant ($P = 0.778$, $n = 36$). However, the PO_4^{3-} availability was 3.5 to 5.5 times higher in the 44-yr site compared to the 4- and >115-yr sites (4-yr, $P = 0.026$; >115 yr, $P = 0.024$). Soil pH was highest in the 4-yr site and decreased logarithmically with time since fire ($P = 0.002$, $R^2 = 0.22$, $n = 37$).

Microbial biomass C and N increased with time since fire (C, $P = 0.008$, $R^2 = 0.16$, $n = 37$; N, $P = 0.016$, $R^2 = 0.13$, $n = 37$). However, we were only able to detect marginally significant differences in microbial biomass C and unable to detect significant differences in microbial biomass N among sites (ANOVA, $P = 0.079$ and $P = 0.101$, respectively; Table 1). Microbial biomass C to N mass (C:N) ratio also did not change across the sites ($P = 0.105$). Microbial biomass C normalized by SOC (specific biomass) differed among sites ($P = 0.017$), with specific biomass 36% lower in the 4-yr site compared to the 25-yr site (the largest difference between sites, $P = 0.023$, Fig. 4b).

Extracellular enzyme activity

For all extracellular enzymes assayed, activities normalized by soil mass at the plot scale increased with time since fire (BG, $P < 0.001$, $R^2 = 0.62$, $n = 37$; NAG, $P < 0.001$, $R^2 = 0.55$, $n = 37$; AP, $P < 0.001$, $R^2 = 0.68$, $n = 37$; Fig. 5a–c). However, there were significant interactions with sample date for BG and AP ($P < 0.001$), indicating that differences in activity among chronosequence sites were only apparent during the June (wet) sampling date. During the dry season sampling date, enzyme activities were consistently low. For the June sampling date, the 4-yr site was, on average, 70–80% lower than the >115-yr site for the assayed extracellular enzymes ($P < 0.001$). Even in the 44-yr site, NAG and AP were still 69% and 58% lower than >115-yr site, respectively (NAG, $P < 0.001$; AP, $P = 0.016$). Activity for BG in the 44-yr site was only marginally lower than the >115-yr site ($P = 0.077$, -39%). However, for BG and AP, the 25-yr site was not significantly different from the >115-yr site ($P = 0.933$ and $P = 0.279$, respectively).

Extracellular enzyme activities during the June sampling date normalized by microbial biomass increased logarithmically with time since fire (BG, $P = 0.032$, $R^2 = 0.10$, $n = 37$, Fig. 4c; NAG, $P = 0.024$, $R^2 = 0.11$, $n = 37$, Appendix S1: Fig. S1a; AP, $P = 0.001$, $R^2 = 0.24$, $n = 37$, Appendix S1: Fig. S1b). The biomass-normalized enzyme activity for BG and AP was almost half in the 4-yr site compared to all other sites ($P < 0.05$). However, for NAG, the 13- through 44-yr sites were not significantly different from the 4-yr site (13 yr, $P = 0.130$; 25 yr, $P = 0.977$; 44 yr, $P = 0.781$), while the >115-yr site was significantly higher ($P = 0.033$).

Extracellular enzyme activity normalized by SOC showed similar patterns, increasing with time since fire for the June sampling date. However, while BG normalized by SOC increased logarithmically through the first 44 yr ($P < 0.001$, $R^2 = 0.33$, $n = 37$), the 4-yr site was not significantly different from the >115-yr site ($P = 0.121$, Appendix S1: Fig. S2a). Both NAG and AP activities normalized by SOC increased logarithmically with time since fire (NAG, $P < 0.001$, $R^2 = 0.20$, $n = 37$, Appendix S1: Fig. S2b; AP, $P < 0.001$, $R^2 = 0.27$, $n = 37$, Appendix S1: Fig. S2c).

Microbial activity

At the plot scale, cumulative respiration increased with time since fire ($P < 0.001$, $R^2 = 0.34$, $n = 37$) but interacted significantly with sample date ($P < 0.001$; Fig. 6a), indicating that differences in respiration among chronosequence sites were only apparent during the June sampling date. For the June sampling date, respiration was, on average, 65% lower for the 4–44 yr sites compared to the >115-yr site; however, the reduction was not significant in the 25-yr site ($P = 0.158$, $P < 0.05$ for the other three sites). On average, the September sampling date had 25–63% lower respiration rates than the June sampling date ($P = 0.002$), with the greatest reductions in the >115-yr site. June respiration normalized by SOC and MBC did not change with time since fire ($P = 0.778$

NICHOLAS C. DOVE ET AL.

TABLE 1. Mean (with SE) plot-scale soil properties of the chronosequence sites and coefficients of determination (r^2) of the positive (+) or negative (-) correlation with time since fire ($n = 37$).

Property	Time since fire (yr)					Time Since fire r^2
	4	13	25	44	>115	
Soil C (%)	7.81[a] (0.91)	4.36[a] (0.50)	6.42[a] (1.81)	6.35[a] (0.72)	14.25[b] (2.69)	+0.32
Soil N (%)	0.38 [ab] (0.05)	0.17[a] (0.02)	0.29[ab] (0.06)	0.30[ab] (0.04)	0.56[b] (0.12)	+0.14†
Soil C:N	25.0[a] (0.9)	30.0[bc] (0.6)	27.6[abc] (1.16)	25.2[ab] (0.5)	31.3[c] (1.8)	+0.13‡
DOC (K$_2$SO$_4$-extractable; mg/kg)	205[ab] (34)	91[a] (10)	144[a] (27)	135[a] (19)	300[b] (48)	+0.19‡
DON (total − KCl-extractable; g/kg)	3.76[b] (0.50)	1.72[a] (0.21)	2.87[ab] (0.63)	3.03[ab] (0.40)	5.56[b] (1.18)	+0.14‡
Microbial biomass C (mg/kg)	427 (71)	317 (44)	483 (66)	420 (75)	710 (156)	+0.16
Microbial biomass N (mg/kg)	54.2 (8.0)	50.6 (7.6)	85.9 (14.8)	71.3 (14.6)	104.0 (24.3)	+0.13§
Microbial C:N	8.51 (0.91)	6.45 (0.19)	6.32 (0.68)	6.63 (0.73)	6.72 (0.56)	N.S.¶
Wet season NH$_4^+$ (mg·kg^{-1} resin·d^{-1})#	0.092[b] (0.037)	0.031[ab] (0.001)	0.051[ab] (0.012)	0.015[a] (0.002)	0.036[ab] (0.011)	N.S.
Dry season NH$_4^+$ (mg·kg^{-1} resin·d^{-1}) ‖	0.165[b] (0.038)	0.274[b] (0.128)	0.142[ab] (0.050)	0.107[ab] (0.023)	0.058[a] (0.006)	N.S.
Wet season NO$_3^-$ (mg·kg^{-1} resin·d^{-1})	4.002[b] (1.589)	0.031[a] (0.001)	0.051[a] (0.030)	0.063[a] (0.030)	0.248[a] (0.116)	N.S.
Dry season NO$_3^-$ (mg·kg^{-1} resin·d^{-1})	0.102 (0.045)	0.040 (0.002)	0.040 (0.002)	0.052 (0.005)	0.040 (0.009)	N.S.
Wet season PO$_4^{3-}$ (µg·kg^{-1} resin·d^{-1})	0.2[a] (0.1)	65.1[b] (25.2)	11.8[b] (1.0)	19.5[b] (1.2)	182.0[b] (43.6)	+0.53§
Dry season PO$_4^{3-}$ (µg·kg^{-1} resin·d^{-1})	17.6[a] (2.9)	45.1[ab] (5.0)	21.9[ab] (2.0)	78.0[b] (14.8)	12.1[a] (1.28)	N.S.
pH$_{H2O}$	6.49[c] (0.10)	6.18[bc] (0.14)	5.92[ab] (0.06)	5.71[a] (0.10)	5.99[ab] (0.12)	−0.30
pH$_{0.01 \ M \ CaCl2}$	5.57[b] (0.08)	4.83[a] (0.14)	4.73[a] (0.09)	4.53[a] (0.09)	4.97[a] (0.17)	−0.22*
WHC (kg/kg) ††	0.81[a] (0.05)	0.83[a] (0.10)	0.83[a] (0.10)	0.76[a] (0.09)	1.38[b] (0.18)	+0.31†
Soil MAT (°C) ‡‡	12.6 (0.9)	12.7 (0.2)	11.3 (1.0)	10.6 (0.1)	9.4 (0.7)	−0.26
Growing season mean temperature (°C) §§	17.33 (1.6)	18.5 (0.1)	16.7 (1.3)	15.0 (0.3)	12.7 (0.7)	−0.37

Note: Letters represent significant differences among sites (ANOVA; $\alpha = 0.05$).
*Log of independent variable.
† Natural-log-transformation of the independent variable.
‡ Natural-log-transformation of the dependent variable.
§ Natural-log-transformation of the independent and dependent variable.
¶ Not significant (P > 0.05).
# November–June.
‖ June–September.
†† Water holding capacity.
‡‡ Mean annual temperature.
§§ May–December.

and $P = 0.226$, respectively, data not shown), resulting in respiration being positively correlated with SOC concentrations ($r = 0.85$, $P < 0.001$, $n = 115$, Fig. 4c).

Net methane emissions were unaffected by time since fire ($P = 0.201$) and sample date ($P = 0.806$, Fig. 6b). Nitrous oxide emissions increased logarithmically with time since fire ($P < 0.001$, $R^2 = 0.29$, $n = 37$) and were unaffected by sample date ($P = 0.911$, Fig. 6c). Averaged for both sample dates, nitrous oxide emissions in the 4-yr site were 10% of the >115-yr site ($P = 0.036$), but the 13-yr site was not significantly different from the >115-yr site ($P = 0.567$).

N transformations

At the plot scale, net N mineralization and nitrification were highest in the 4-yr fire site and decreased

logarithmically with time since fire (net N mineralization, $P < 0.001$, $R^2 = 0.30$, $n = 37$; net nitrification, $P < 0.001$, $R^2 = 0.22$, $n = 37$; Fig. 7a, b). However, there were significant interactions with sample date for both net N mineralization and net nitrification ($P = 0.003$ and $P = 0.033$, respectively). Differences in net N mineralization and net nitrification during the incubation were dampened for samples collected at the end of the dry season (i.e., September). At this sampling date, there were higher net rates of N transformations in the >115-yr site compared to the June sampling date. During the wet season sampling date (i.e., June), net N mineralization decreased logarithmically from 0.96 ± 0.16 mg N·kg^{-1}·d^{-1} (mean ± SE) in the 4-yr site to 0.10 ± 0.17 mg N·kg^{-1}·d^{-1} in the >115-yr site, and net nitrification in the 4-yr site was six times higher than the >115-yr site (1.24 vs. 0.27 mg N·kg^{-1}·d^{-1}). For the June
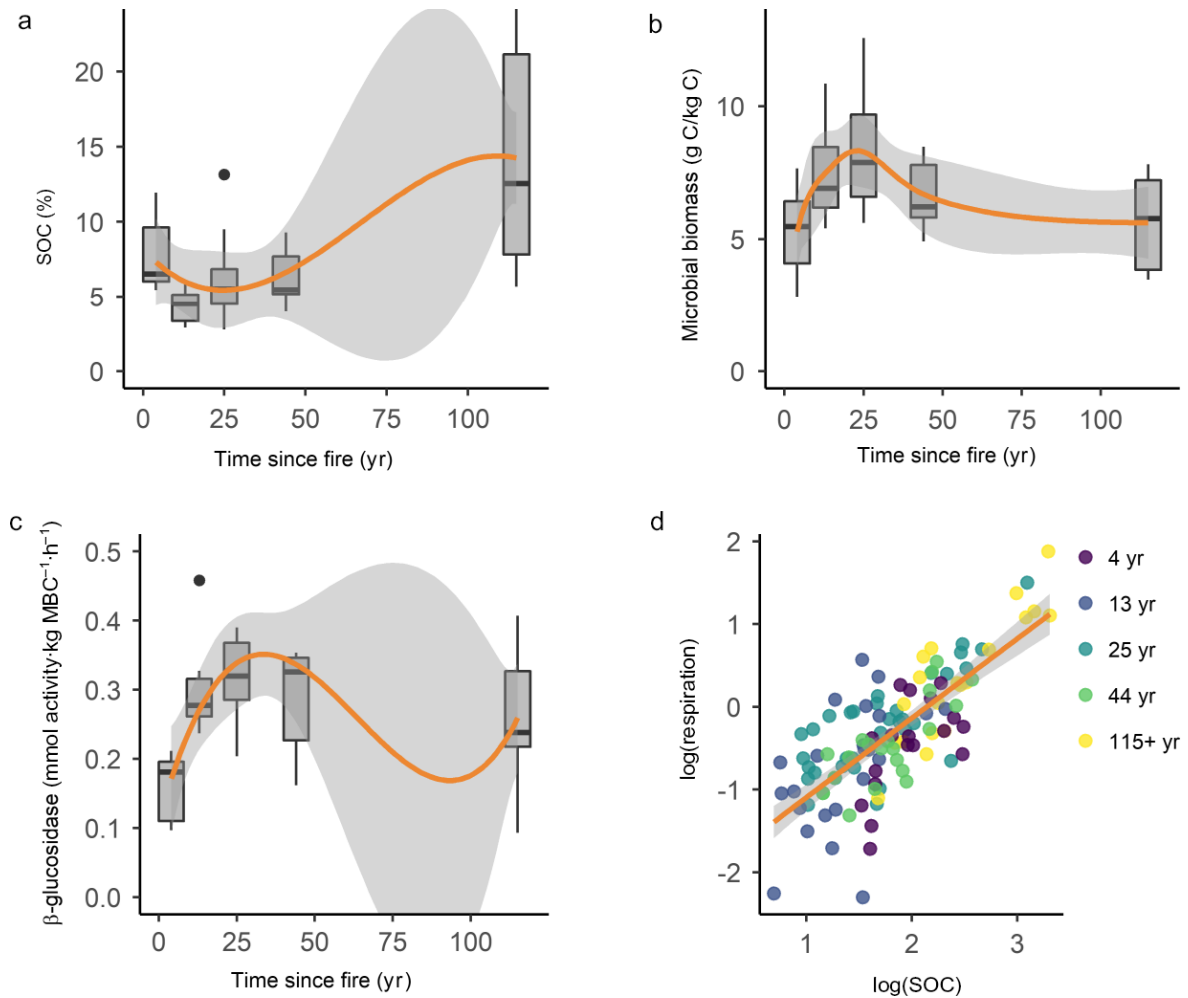
FIG. 4. Control of carbon (C) cycling processes in the long-term recovery after fire. (a) June plot-scale soil organic C (SOC; orange line represents third-order polynomial linear regression, $P < 0.001$, $R^2 = 0.35$) plotted against time since fire, (b) microbial biomass C (MBC) normalized by SOC against time since fire, (c) β-glucosidase normalized by MBC (orange line represents second-order polynomial linear regression, $P = 0.012$, $R^2 = 0.18$) plotted against time since fire, and (d) sample-scale respiration (measured as mg CO_2-C/kg) as a function of SOC quantity (orange line shows best-fit regression, $P < 0.001$, $R^2 = 0.56$, $n = 114$). For all panels, shaded region shows the 95% confidence interval of the best-fit regression. For plot-scale measurements (a, b, and c), $n = 6$ in the 13-yr site, $n = 7$ in the 44-yr site, and $n = 8$ in all other sites.

sampling date, both net N mineralization and nitrification were significantly higher in the 4-yr site compared to the >115-yr site (both: $P < 0.001$), but the 13-yr through 44-yr sites were not significantly different from the >115-yr site ($P > 0.100$). Overall, net N mineralization and nitrification were highly correlated (Spearman's rho = 0.90, $P < 0.001$, $n = 116$).

At the plot-scale, soil nitrification potential showed a non-monotonic response to time since fire ($P < 0.001$; Fig. 7c), with the highest potentials in the 44-yr site. Nitrification potential at this site was about 3.5 times higher than the 13-yr ($P = 0.002$) and >115-yr sites ($P < 0.001$). The 4- and the 25-yr sites were also 2 and 1.5 times higher than the >115-yr site, respectively (both $P < 0.001$). Nitrification potential was unaltered by the main effect of sample date ($P = 0.109$), and this trend was consistent across both sampling dates (i.e., no interaction; $P = 0.300$).

Influence of cover type

Cover type was not a consistent predictor of biogeochemical processes (Table 2, Appendix S1: Figs. S3–S5). However, microbial respiration and net nitrification significantly differed by cover type ($P = 0.024$ and $P = 0.033$, respectively). Upon further inspection using Tukey's HSD tests, microbial respiration under N-fixing plants was marginally higher than under the bare cover type (30%, $P = 0.082$), but we failed to detect even marginally significant differences among cover
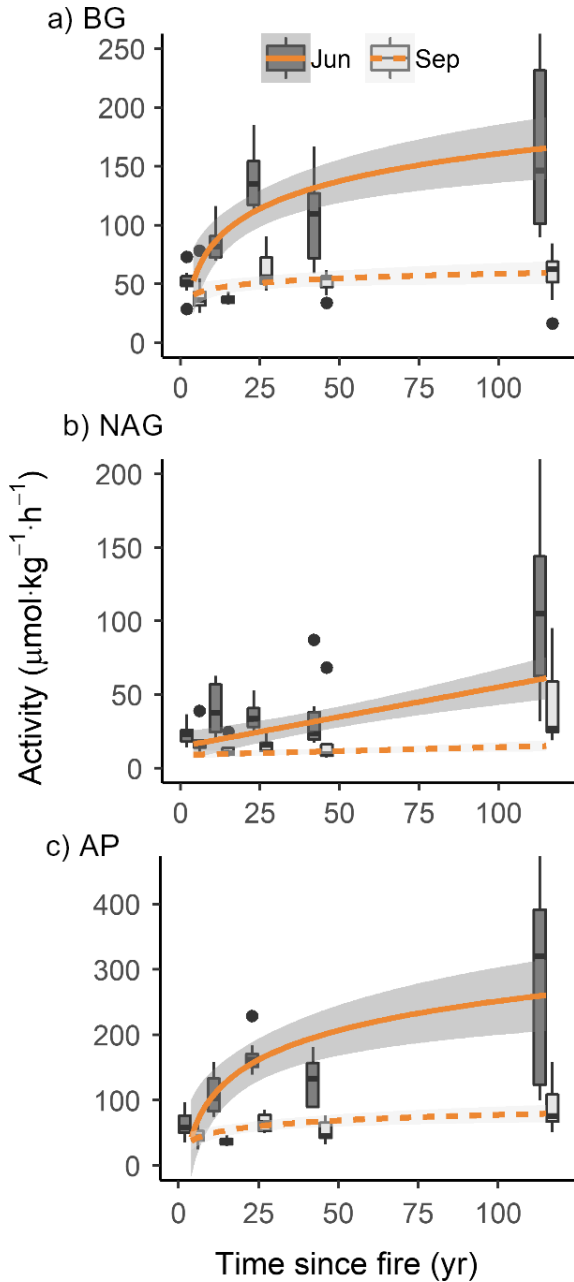
FIG. 5. Plot-scale extracellular enzyme activity for (a) β-glucosidase (BG), (b) N-acetylglucosaminidase (NAG), and (c) acid phosphatase (AP) with time since fire (13-yr site, $n = 6$; 44-yr site, $n = 7$; all other sites, $n = 8$). Gray and white box plots represent the median, interquartile range (IQR), and $1.5 \times$ IQR for enzyme activities at each chronosequence site during June and September, respectively. Orange lines show the best-fit regression of extracellular enzyme activity with time since fire, and shaded area shows the 95% confidence interval of the regression.

FIG. 6. Plot-scale cumulative gas fluxes for (a) carbon dioxide (CO_2), (b) methane (CH_4), and (c) nitrous oxide (N_2O) from 31-d laboratory incubations (13-yr site, $n = 6$; 44-yr site, $n = 7$; all other sites, $n = 8$). Gray and white box plots represent the median, interquartile range (IQR), and $1.5 \times$ IQR for gas fluxes at each chronosequence site during June and September, respectively. Orange lines show the best-fit regression of gas emissions with time since fire, and shaded area shows the 95% confidence interval of the regression. There was no statistically significant interaction between sample date and time since fire for CH_4 and N_2O fluxes, so for these response variables, only one regression line is shown.

types for net nitrification due to the loss of degrees of freedom and inferential power when assessing multiple comparisons. There was also a significant cover type by time since fire interaction for N_2O emissions
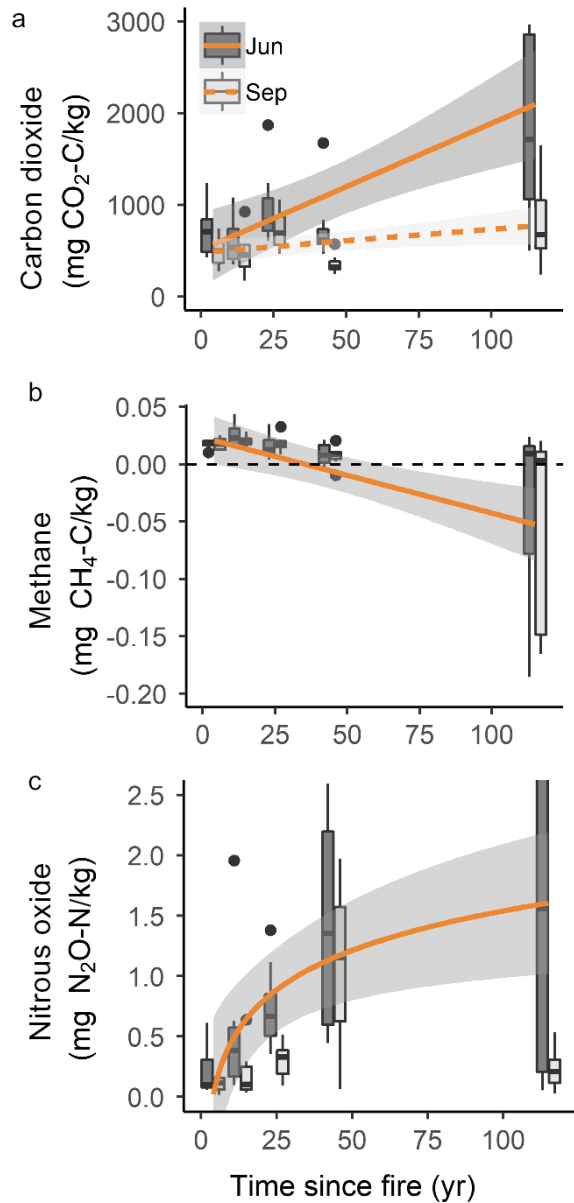
($P = 0.040$). In the 44-yr site, N_2O emissions were, on average, 10 times higher under N-fixing plants compared to trees, although this was only marginally significant ($P = 0.075$). There was a similar difference in
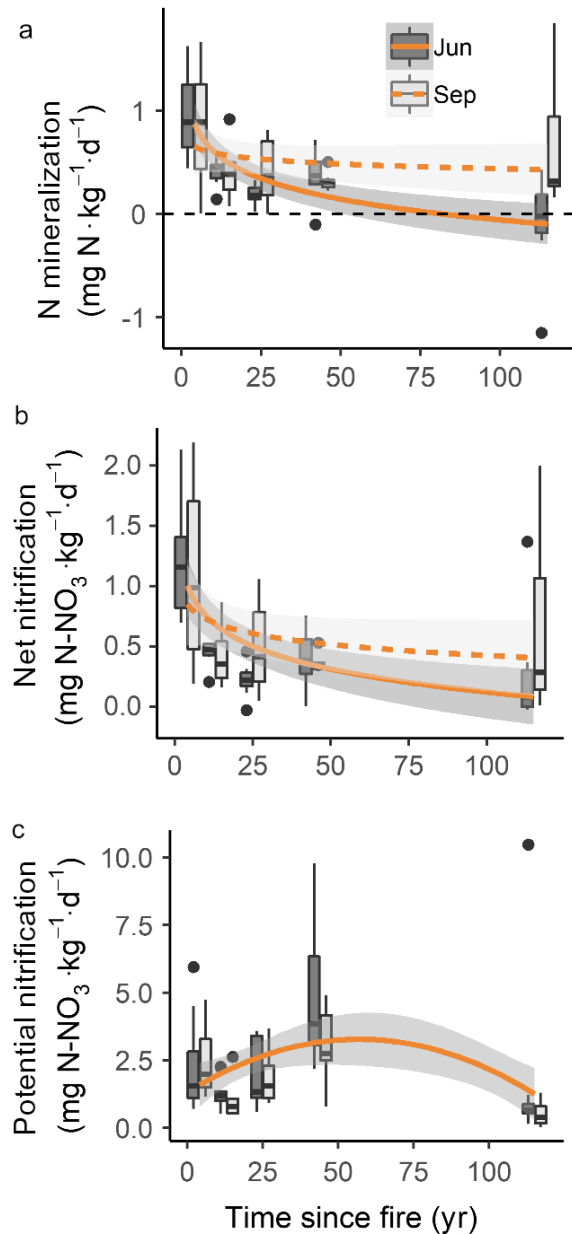
Fig. 7. Plot-scale net nitrogen (N) (a) mineralization and (b) net nitrification during a 31-d laboratory incubation, and potential nitrification (c, 13-yr site, $n = 6$; 44-yr site, $n = 7$; all other sites, $n = 8$). Gray and white box plots representing the median, interquartile range (IQR), and $1.5 \times$ IQR for N transformations at each chronosequence site during June and September, respectively. Orange lines show the best-fit regression of N transformations with time since fire, and shaded area shows the 95% confidence interval of the regression. There was no statistically significant interaction between sample date and time since fire for nitrification potential, so for this response variable, only one regression line is shown.

the 25-yr site with soils under N-fixing plants producing, on average, 10 times higher N_2O emissions than bare soils, but again this was only marginally different ($P = 0.058$).

DISCUSSION

Multi-decadal impacts on C cycling

Consistent with our hypothesis, ecologically novel, high-severity fire resulted in multi-decadal alterations to the C cycle, specifically, decreased mineral SOC (Table 1), soil extracellular enzyme activity (Fig. 5), and soil microbial respiration (Fig. 6a), and the controls on C cycling (particularly soil microbial respiration) changed with time. Whereas combustion of the organic soil horizon is common, generally, losses of mineral SOC from fire are rare. In a global meta-analysis encompassing 57 publications across both prescribed fire and wildfire, post-fire mineral SOC concentrations decreased by 11% (Nave et al. 2011). Mineral SOC is more resistant to combustion compared to organic horizon C due to the high heat capacity of mineral soil (Neary et al. 1999). Hence, higher-severity fire patches have been shown to result in greater mineral soil C losses compared to low-severity patches in southern boreal forests (Kolka et al. 2014). Even under high-severity wildfire, other sites in the Sierra Nevada and similar dry coniferous forests did not have significant decreases in mineral SOC 3–30 yr following fire compared to unburned sites (Johnson et al. 2005, Grady and Hart 2006, Kaye et al. 2010, Ross et al. 2012, Adkins et al. 2019). However, there were, on average, 20% decreases in soil C regardless of burn severity directly after fire across five mixed-conifer sites in California when the site was assessed pre/post-fire (Miesel et al. 2018). This difference highlights the nuanced congruence between fire severity and mineral SOC loss, the importance of time since fire, and potential differences between experimental and retrospective studies. Our long-term (>20 yr) reduction in mineral SOC compared to unburned sites has, to the best of our knowledge, not been described by the literature. In another high-severity wildfire chronosequence in a Mediterranean *Pinus* forest, mineral SOC recovered 12 yr post-fire after an initial decrease (Kavdır et al. 2005). The scarcity of long-term high-severity fire chronosequences prevents a global interpretation of the long-term effects of high-severity fire on SOC pools and underscores the importance of long-term fire ecology research.

Surprisingly, wet season respiration normalized by SOC, which is an index of C quality and availability (Grady and Hart 2006, Rousk and Frey 2015), was unaffected by fire. Pyrolization of organic matter results in an increase in aromatic compounds that are generally more resistant to microbial decay (Keiluweit et al. 2010, Bird et al. 2015). Frequently, this results in decreased respiration (Grady and Hart 2006, Santos et al. 2012, Whitman et al. 2016). However, because wet season respiration in our study was positively correlated with SOC concentrations (Fig. 4c), it is likely that long-term decreased C quantity, not quality or accessibility, decreased rates of respiration throughout the first four decades post-fire (Fig. 4a).

TABLE 2. Sample-scale summary statistics (P) for the influence of time since fire and substratum cover type on biogeochemical processes using analysis of variance.

Processes	Time since fire	Cover type	Interaction
Microbial activity			
CO_2 (mg C-CO_2/kg)	**<0.001**	**0.024**	0.616
CH_4 (mg C-CH_4/kg)	**<0.001**	0.652	0.775
N_2O (mg N-N_2O/kg)	**0.001**	0.077	**0.040**
Exo-enzymes activities			
β-glucosidase (μmol/kg)	**<0.001**	0.119	0.459
N-acetylglucosaminidase (μmol/kg)	**<0.001**	0.560	0.969
Acid phosphatase (μmol/kg)	**<0.001**	0.213	0.072
N transformations			
Net N mineralization (mg N/kg)	**<0.001**	0.056	0.288
Net nitrification (mg N-NO_3^-/kg)	**<0.001**	**0.033**	0.494
Nitrification potential (mg N-NO_3^-/kg)	**<0.001**	0.367	0.888

Note: Values in boldface type are considered significant ($\alpha = 0.05$).

In the short-term (<10 yr), decreased soil microbial biomass and activity likely also decreased microbial respiration. While microbial biomass on a soil mass basis was only marginally significantly affected by fire, the fraction of SOC as microbial biomass C was lowest in the 4-yr fire site (Fig. 4b). This suggests that there were indirect effects of fire on biomass growth besides C, such as altered soil structure, decreases in the quality of litter inputs, or reductions in other limiting resources (e.g., PO_4^{3-} availability was lowest in the 4-yr site, Table 1). Alternatively, fire-induced microbial mortality may still have had a lingering effect 4 yr post-fire, as there was less microbial biomass C than would be expected per mass of total C. Additionally, wet season extracellular enzyme activity expressed on a microbial biomass basis and on a soil mass basis increased with time since fire (Fig. 4a), suggesting that the microbial communities were less active immediately post-fire. Enzyme activities generally are lower in burned sites than in unburned controls (Guénon et al. 2013, Knelman et al. 2015, 2017). However, activities normalized by microbial biomass are often not reported. Thus, it is unclear if published patterns are in response to decreased microbial biomass or altered edaphic conditions that decrease activity. For instance, increased soil pH (seen in the 4-yr site, Table 1) can have a negative effect on soil extracellular enzyme activity (Sinsabaugh et al. 2008, Kivlin and Treseder 2014) because the pH optima for many extracellular enzymes is ~5 (Leprince and Quiquampoix 1996, Turner 2010). Therefore, short-term changes in soil conditions along with decreased soil microbial biomass lowered soil enzyme activity and likely dampened microbial respiration (Fig. 4a–c).

Consistent methane efflux among time since fire sites is largely at odds with other studies that show that in situ methane uptake increases at least 10 yr post-fire in semiarid ecosystems (Gathany and Burke 2001, Sullivan et al. 2011). Whereas decreased plant cover altered soil moisture and temperature dynamics, which impact methane dynamics (Segers 1998), the presence of an O horizon and ability of methane to diffuse into the mineral soil is the greatest driver of methane uptake (Sullivan et al. 2011). However, unlike these previous studies, we measured methane efflux under laboratory conditions, controlling for water potential (i.e., soils were incubated at WHC) and temperature and disrupting the original soil structure. Our findings show that *potential* methane uptake slightly increases with time since fire, possibly due to the recovery of the methane-oxidizer community. There are relatively few studies describing methane dynamics post-fire in semiarid ecosystems. Given that methane is an important greenhouse gas, which may change with wildfire, and that semiarid ecosystems are projected to burn more frequently (Westerling et al. 2006, Restaino and Safford 2018), future studies of the C cycle in response to wildfire should include methane dynamics.

Short-term impacts on N cycling caused by increased N availability

Our hypothesis that N cycling processes would be increased by substrate availability shortly after fire (<10 yr) was supported by the data. The drastic increase in N availability after fire in fire-suppressed ecosystems is corroborated by numerous studies (St. John and Rundel 1976, Covington and Sackett 1992, Kaye and Hart 1998, DeLuca and Sala 2006, Johnson et al. 2007, 2008, Kurth et al. 2014), and may be due to fire-induced N mineralization (St. John and Rundel 1976), wetter and warmer conditions that increase mineralization of organic matter (Kaye and Hart 1998), increased cover of N-fixing plants (Johnson et al. 2005), decreased C:N ratio of litter from post-fire vegetation (e.g., grasses; Boyle et al. 2005), or lower plant N uptake post-fire (Kurth et al. 2014). Combined with decreased C availability in the recent fire sites, post-fire N availability likely contributed to a relative decrease in microbial N demand and increased wet season net rates of N mineralization and nitrification possibly through decreased N immobilization (Kaye and Hart 1998).

Our hypothesis that fire-induced changes to N transformations would last longer than one decade was largely unsupported by the data. Whereas others have seen long-term increases in gross, net, and potential nitrification one to three decades post-wildfire in seasonally dry mixed-conifer forests similar to our sites and more globally (DeLuca and Sala 2006, Kurth et al. 2014, Wang et al. 2014), we only detected increased net nitrification and nitrate flux in the 4-yr site and increased nitrification potential in the 44-yr site compared to the >115-yr

site. The lack of correspondence between nitrification potential and net nitrification suggests that net nitrification was unaltered by changes to the nitrifier population size (to which nitrification potential is directly related; Belser 1979). Furthermore, N_2O efflux (which we used as a measure of nitrifier activity given soils were incubated under putative aerobic conditions) increased with time since fire and was also uncorrelated with both net nitrification and nitrification potential. This suggests that differences in the microsite heterogeneity of ammonium availability among sites caused variations in NO_3^- consumption further uncoupling gross and net rates of nitrification (Davidson et al. 1990). High rates of NO_3^- consumption in mature forests (with relatively high N demand like our >115-yr site) has been shown to mask gross nitrification in mature forest soils (Stark and Hart 1997), so it is not necessarily surprising that these three indices of the nitrifier community were uncorrelated among sites with vastly different C and N availabilities.

The relatively low rates of potential nitrification and N_2O efflux at the 4- through 25-yr sites could be due to longer term decreases in population of ammonia oxidizers (Yeager et al. 2005, but see Long et al. 2014), which are more sensitive to heat compared to heterotrophic bacteria (Dunn et al. 1985). Differences in the recovery of ammonia-oxidizing archaea (AOA) and ammonia-oxidizing bacteria (AOB) could also drive the response of nitrification potential and nitrification-derived N_2O emissions, as AOB show a stronger relationship with nitrification potentials (Carey et al. 2016) and are relatively more "leaky" in terms of N_2O emissions during nitrification (Di et al. 2010). Therefore, further analysis of the microbial community might help elucidate different patterns of post-fire N cycling among studies.

Influence of cover type

Our hypothesis that the long-term recovery of soil biogeochemical processes would be controlled by vegetative cover type was largely unsupported. In a few instances, rates of biogeochemical processes were greater under N-fixing plants (i.e., microbial respiration and N_2O emissions); however, we found no evidence of cover type becoming more important with time since fire. This is largely at odds with the previous literature describing the recovery of biogeochemical processes following historical fires, which suggests that C and N inputs from recovering vegetation structure the microbial community composition and function (Hart et al. 2005). For instance, grass patches resulting from forest restoration treatments (which include prescribed burning) increase net rates of N transformations and enzyme activities and influence community-level physiological profiles likely through the supply of low C:N ratio plant litter (Kaye and Hart 1998, Boyle et al. 2005). Furthermore, the increase in N-fixing plant (e.g., *Ceanothus* spp.) abundance following wildfire has been linked with increased SOC and microbial activity (Johnson et al. 2005). These

inputs may also interact with microbial processes, as increased shrub cover during secondary succession has been linked to greater concentrations of phenolic compounds which may inhibit nitrification (MacKenzie et al. 2004). Recovering vegetation may also affect N and water availability through plant demand for these soil resources. In the first year after high-severity fire in a ponderosa pine (*Pinus ponderosa*) ecosystem, soils underneath the herb golden corydalis (*Corydalis aurea*) had higher levels of microbial biomass and soil N and lower levels of NH_4^+ and moisture than bare soils (Knelman et al. 2015). Our results demonstrate that plant cover type may not affect the recovery of biogeochemical processes after fire in all contexts.

It is possible that the effect of ecologically novel, high-severity fire was so great that it masked the influence of post-fire vegetation. Post-fire vegetation likely affects soil microorganisms and biogeochemical function through changes to the supply of C through litter and belowground inputs (e.g., net primary production), the quality of C (e.g., percent lignin, C:N ratio), competition for nutrients between the plant and microbial communities, and direct symbioses (e.g., mycorrhizae; Hart et al. 2005). However, mineral SOC concentrations only differed by fire not cover type, and C quality assessed by SOC-normalized respiration was similar regardless of fire and cover type. While post-fire plant C inputs may vary among cover types, these inputs are likely much smaller than the relatively large C pool combusted by these high-severity wildfires.

It is also possible that these vegetation effects emerge at different scales not sampled in our study. Rhizosphere microorganisms are often controlled by the species they have colonized (Bais et al. 2006); however, we did not differentiate between rhizosphere and bulk soil under each cover type. Also, the influence of vegetation can extend several meters into the surrounding bulk soil (Saetre 1999). Hence, patterns may emerge at the rhizosphere, stand, or plot scale (Kaye and Hart 1998, Boyle et al. 2005, Hart et al. 2005) but not the soil-core scale (as in our study). Our plot-scale measurements were an integration of all cover types found in the plot, so we were not able to test a cover-type effect at the plot scale. The emergence of ecological phenomena at different scales is common and underscores the need for multiscale approaches (Levin 1992). Whereas many biochemical transformations occur at microscopic scales, plants likely operate on scales orders of magnitude larger. Hence, understanding the interactions within the plant–soil–microbe system necessitates research at multiple scales, both spatial and temporal.

Seasonal dynamics of biogeochemical rates

Consistent with our hypothesis, differences among fire sites for a majority of the biogeochemical rates were only apparent in the wet season. The Sierra Nevada of California has a Mediterranean-type climate and is

characterized by cool, wet winters and warm, relatively dry summers. During the dry late-summer months, soil microorganisms enter a state of relative dormancy (Lennon and Jones 2011). Hence, rates of extracellular enzyme activity measured at field moisture and CO_2 efflux measured under non-water-limiting conditions were consistently low across all sites. However, net rates of N mineralization and nitrification were consistently higher across all sites when sampled during the dry season. This indicates that soil microorganisms were still mineralizing organic matter, but likely with decreased N immobilization, suggesting that maintenance rather than growth was favored under these conditions. These findings further exemplify how microbial dormancy affects biogeochemical cycles (Hart et al. 1992, Stark and Firestone 1995, Schimel et al. 2007) and that the season during which soils are sampled can affect the ability to detect changes among treatments.

Conclusion and Management Applications

Previous studies suggest that soil biogeochemical processes are generally resilient to wildfire within the historical range of variation for that ecosystem. However, we show that impacts of fire can be long-lasting in instances of disturbances outside the historic range of variation (over twice the historical fire return interval for these forests, Fry et al. 2014). Our data suggest that high-severity wildfires have both short- and long-term implications. The transition from microbial biomass limitation of respiration at early stages of recovery to SOC limitation at later stages of recovery suggests the changing controls of biogeochemical processes post-fire and underscores the importance of long-term fire ecology research. Whereas fire chronosequences may suffer from site-specific characteristics that cannot be controlled for (e.g., micro-scale variations in soil properties) or climatic events that are time dependent (e.g., El Niño events), we show the utility of this approach when sites are carefully selected for common characteristics and when recovery from disturbances occur over long timescales.

At large spatial scales, high-severity fires in the mixed-conifer forests of the Sierra Nevada have numerous negative impacts on human health and ecosystem services. Prescribed burns, selective thinning, and fires managed for resource benefits can help prevent ecologically novel, predominantly high-severity fires (Safford et al. 2009). Hence, these management techniques could be useful in maintaining ecosystem services in the face of climate change and increasing fire severity in dry coniferous forests of the Sierra Nevada and elsewhere. For instance, little if any mineral SOC is combusted during prescribed or low-severity fire in coniferous forests (Boerner et al. 2009, Ryu et al. 2009, Nave et al. 2011, Pellegrini et al. 2018) in contrast to 20% loss during high-severity fire (Miesel et al. 2018). The long-term 45–69% decreases in mineral SOC, relative to the unburned site, found in our study are uncommon; however, areas burning at high severity are proportionally increasing over time (Miller et al. 2009b, Steel et al. 2018) along with fire frequency (Westerling et al. 2006). Therefore, these "rare" occurrences are becoming more common, putting large SOC pools found in temperate coniferous forests at risk. Our results suggest that sustainable forest management in the mixed-conifer forests of the Sierra Nevada should prioritize mitigation of ecologically novel, high-severity fire through prescribed burns, selective thinning, and wildland use fires.

Literature Cited

Adams, M. A. 2013. Mega-fires, tipping points and ecosystem services: Managing forests and woodlands in an uncertain future. Forest Ecology and Management 294:250–261.

Adkins, J., J. Sanderman, and J. Miesel. 2019. Soil carbon pools and fluxes vary across a burn severity gradient three years after wildfire in Sierra Nevada mixed-conifer forest. Geoderma 333:10–22.

Bais, H. P., T. L. Weir, L. G. Perry, S. Gilroy, and J. M. Vivanco. 2006. The role of root exudates in rhizosphere interactions with plants and other organisms. Annual Review of Plant Biology 57:233–266.

Barton, K. 2018. MuMIn: Multi-model inference. https://cran.r-project.org/web/packages/MuMIn/index.html

Bates, D., M. Maechler, B. Bolker, and S. Walker. 2015. Fitting linear mixed-effects models using lme4. Journal of Statistical Software 67:1–48.

Beck, T., R. G. Joergensen, E. Kandeler, F. Makeschin, E. Nuss, H. R. Oberholzer, and S. Scheu. 1997. An interlaboratory comparison of ten different ways of measuring soil microbial biomass C. Soil Biology and Biochemistry 29:1023–1032.

Bell, C. W., B. E. Fricks, J. D. Rocca, J. M. Steinweg, S. K. McMahon, and M. D. Wallenstein. 2013. High-throughput fluorometric measurement of potential soil extracellular enzyme activities. Journal of Visualized Experiments 81: e50961. https://doi.org/10.3791/50961

Belser, L. W. 1979. Population ecology of nitrifying bacteria. Annual Review of Microbiology 33:309–333.

Binkley, D., and S. C. Hart. 1989. The components of nitrogen availability assessments in forest soils. Pages 57–112 in B. A. Stewart, editor. Advances in soil science. Springer, New York, New York, USA.

Binkley, D., and P. Matson. 1983. Ion exchange resin bag method for assessing forest soil nitrogen availability. Soil Science Society of America Journal 47:1050.

Bird, M. I., J. G. Wynn, G. Saiz, C. M. Wurster, and A. McBeath. 2015. The pyrogenic carbon cycle. Annual Review of Earth and Planetary Sciences 43:273–298.

Boerner, R. E. J., J. A. Brinkman, and A. Smith. 2005. Seasonal variations in enzyme activity and organic carbon in soil of a

burned and unburned hardwood forest. Soil Biology and Biochemistry 37:1419–1426.

Boerner, R. E. J., C. Giai, J. Huang, and J. R. Miesel. 2008. Initial effects of fire and mechanical thinning on soil enzyme activity and nitrogen transformations in eight North American forest ecosystems. Soil Biology and Biochemistry 40:3076–3085.

Boerner, R. E. J., J. Huang, and S. C. Hart. 2009. Impacts of Fire and Fire Surrogate treatments on forest soil properties: a meta-analytical approach. Ecological Applications 19:338–358.

Bohlman, G. N., M. North, and H. D. Safford. 2016. Shrub removal in reforested post-fire areas increases native plant species richness. Forest Ecology and Management 374:195–210.

Boyle, S. I., S. C. Hart, J. P. Kaye, and M. P. Waldrop. 2005. Restoration and canopy type influence soil microflora in a ponderosa pine forest. Soil Science Society of America Journal 69:1627–1638.

Brookes, P. C., A. Landman, G. Pruden, and D. S. Jenkinson. 1985. Chloroform fumigation and the release of soil nitrogen: A rapid direct extraction method to measure microbial biomass nitrogen in soil. Soil Biology and Biochemistry 17:837–842.

Burns, R. G., J. L. DeForest, J. Marxsen, R. L. Sinsabaugh, M. E. Stromberger, M. D. Wallenstein, M. N. Weintraub, and A. Zoppini. 2013. Soil enzymes in a changing environment: current knowledge and future directions. Soil Biology and Biochemistry 58:216–234.

Butler, O. M., J. J. Elser, T. Lewis, B. Mackey, C. Chen, and S. Niu. 2018. The phosphorus-rich signature of fire in the soil–plant system: a global meta-analysis. Ecology Letters 21:335–344.

Caon, L., V. R. Vallejo, C. J. Ritsema, and V. Geissen. 2014. Effects of wildfire on soil nutrients in Mediterranean ecosystems. Earth-Science Reviews 139:47–58.

Carey, C. J., N. C. Dove, J. M. Beman, S. C. Hart, and E. L. Aronson. 2016. Meta-analysis reveals ammonia-oxidizing bacteria respond more strongly to nitrogen addition than ammonia-oxidizing archaea. Soil Biology and Biochemistry 99:158–166.

Cottingham, K. L., J. T. Lennon, and B. L. Brown. 2005. Knowing when to draw the line: designing more informative ecological experiments. Frontiers in Ecology and the Environment 3:145–152.

Covington, W. W., and S. S. Sackett. 1992. Soil mineral nitrogen changes following prescribed burning in ponderosa pine. Forest Ecology and Management 54:175–191.

Davidson, E. A., J. M. Stark, and M. K. Firestone. 1990. Microbial production and consumption of nitrate in an annual grassland. Ecology 71:1968–1975.

DeLuca, T. H., and A. Sala. 2006. Frequent fire alters nitrogen transformations in ponderosa pine stands of the inland Northwest. Ecology 87:2511–2522.

Di, H. J., K. C. Cameron, R. R. Sherlock, J.-P. Shen, J.-Z. He, and C. S. Winefield. 2010. Nitrous oxide emissions from grazed grassland as affected by a nitrification inhibitor, dicyandiamide, and relationships with ammonia-oxidizing bacteria and archaea. Journal of Soils and Sediments 10:943–954.

Dillon, G. K., Z. A. Holden, P. Morgan, M. A. Crimmins, E. K. Heyerdahl, and C. H. Luce. 2016. Both topography and climate affected forest and woodland burn severity in two regions of the western US, 1984 to 2006. Ecosphere 2:1–33.

Dunn, P. H., S. C. Barro, and M. Poth. 1985. Soil moisture affects survival of microorganisms in heated chaparral soil. Soil Biology and Biochemistry 17:143–148.

Fest, B., T. Wardlaw, S. J. Livesley, T. J. Duff, and S. K. Arndt. 2015. Changes in soil moisture drive soil methane uptake along a fire regeneration chronosequence in a eucalypt forest landscape. Global Change Biology 21:4250–4264.

Fox, J., and S. Weisberg. 2011. An R companion to applied regression. Second edition. Sage, Thousand Oaks, California, USA.

Fry, D. L., S. L. Stephens, B. M. Collins, M. P. North, E. Franco-Vizcaíno, and S. J. Gill. 2014. Contrasting spatial patterns in active-fire and fire-suppressed Mediterranean climate old-growth mixed conifer forests. PLoS ONE 9:e88985.

Fultz, L. M., J. Moore-Kucera, J. Dathe, M. Davinic, G. Perry, D. Wester, D. W. Schwilk, and S. Rideout-Hanzak. 2016. Forest wildfire and grassland prescribed fire effects on soil biogeochemical processes and microbial communities: two case studies in the semi-arid Southwest. Applied Soil Ecology 99:118–128.

Gathany, M., and I. C. Burke. 2001. Post-fire soil fluxes of CO_2, CH_4 and N_2O along the Colorado Front Range. International Journal of Wildland Fire 20:838–846.

Grady, K. C., and S. C. Hart. 2006. Influences of thinning, prescribed burning, and wildfire on soil processes and properties in southwestern ponderosa pine forests: a retrospective study. Forest Ecology and Management 234:123–135.

Guénon, R., M. Vennetier, N. Dupuy, S. Roussos, A. Pailler, and R. Gros. 2013. Trends in recovery of Mediterranean soil chemical properties and microbial activities after infrequent and frequent wildfires. Land Degradation & Development 24:115–128.

Hanan, E. J., J. P. Schimel, K. Dowdy, and C. M. D'Antonio. 2016. Effects of substrate supply, pH, and char on net nitrogen mineralization and nitrification along a wildfire-structured age gradient in chaparral. Soil Biology and Biochemistry 95:87–99.

Hart, S. C., and M. K. Firestone. 1991. Forest floor-mineral soil interactions in the internal nitrogen cycle of an old-growth forest. Biogeochemistry 12:103–127.

Hart, S. C., M. K. Firestone, and E. A. Paul. 1992. Decomposition and nutrient dynamics of ponderosa pine needles in a Mediterranean-type climate. Canadian Journal of Forest Research 22:306–314.

Hart, S. C., J. M. Stark, E. A. Davidson, and M. K. Firestone. 1994. Nitrogen mineralization, immobilization, and nitrification. Pages 985–1018 In Methods of soil analysis: part 2—microbiological and biochemical properties sssabookseries. Soil Science Society of America, Madison, Wisconsin, USA.

Hart, S. C., T. H. DeLuca, G. S. Newman, M. D. MacKenzie, and S. I. Boyle. 2005. Post-fire vegetative dynamics as drivers of microbial community structure and function in forest soils. Forest Ecology and Management 220:166–184.

Haubensak, K. A., S. C. Hart, and J. M. Stark. 2002. Influences of chloroform exposure time and soil water content on C and N release in forest soils. Soil Biology and Biochemistry 34:1549–1562.

Holden, S. R., B. M. Rogers, K. K. Treseder, and J. T. Randerson. 2016. Fire severity influences the response of soil microbes to a boreal forest fire. Environmental Research Letters 11:035004.

Jennings, T. N., J. E. Smith, K. Cromack, E. W. Sulzman, D. McKay, B. A. Caldwell, and S. I. Beldin. 2012. Impact of postfire logging on soil bacterial and fungal communities and soil biogeochemistry in a mixed-conifer forest in central Oregon. Plant and Soil 350:393–411.

Johnson, D. W., J. F. Murphy, R. B. Susfalk, T. G. Caldwell, W. W. Miller, R. F. Walker, and R. F. Powers. 2005. The effects of wildfire, salvage logging, and post-fire N-fixation on the

nutrient budgets of a Sierran forest. Forest Ecology and Management 220:155–165.

Johnson, D., J. D. Murphy, R. F. Walker, D. W. Glass, and W. W. Miller. 2007. Wildfire effects on forest carbon and nutrient budgets. Ecological Engineering 31:183–192.

Johnson, D. W., M. E. Fenn, W. W. Miller, and C. F. Hunsaker. 2008. Fire effects on carbon and nitrogen cycling in forests of the Sierra Nevada. Pages 405–423 *in* A. Bytnerowicz, M. J. Arbaugh, A. R. Riebau, and C. Andersen, editors. Developments in environmental science. Elsevier, Amsterdam, The Netherlands.

Kavdır, Y., H. Ekinci, O. Yüksel, and A. R. Mermut. 2005. Soil aggregate stability and 13C CP/MAS-NMR assessment of organic matter in soils influenced by forest wildfires in Çanakkale, Turkey. Geoderma 129:219–229.

Kaye, J. P., and S. C. Hart. 1998. Ecological restoration alters nitrogen transformations in a ponderosa pine–bunchgrass ecosystem. Ecological Applications 8:1052–1060.

Kaye, J. P., S. C. Hart, P. Z. Fulé, W. W. Covington, M. M. Moore, and M. W. Kaye. 2005. Initial carbon, nitrogen, and phosphorus fluxes following ponderosa pine restoration treatments. Ecological Applications 15:1581–1593.

Kaye, J. P., J. Romanyà, and V. R. Vallejo. 2010. Plant and soil carbon accumulation following fire in Mediterranean woodlands in Spain. Oecologia 164:533–543.

Keiluweit, M., P. S. Nico, M. G. Johnson, and M. Kleber. 2010. Dynamic molecular structure of plant biomass-derived black carbon (Biochar). Environmental Science & Technology 44:1247–1253.

Kivlin, S. N., and K. K. Treseder. 2014. Soil extracellular enzyme activities correspond with abiotic factors more than fungal community composition. Biogeochemistry 117:23–37.

Knelman, J. E., E. B. Graham, N. A. Trahan, S. K. Schmidt, and D. R. Nemergut. 2015. Fire severity shapes plant colonization effects on bacterial community structure, microbial biomass, and soil enzyme activity in secondary succession of a burned forest. Soil Biology and Biochemistry 90:161–168.

Knelman, J. E., E. B. Graham, S. Ferrenberg, A. Lecoeuvre, A. Labrado, J. L. Darcy, D. R. Nemergut, and S. K. Schmidt. 2017. Rapid shifts in soil nutrients and decomposition enzyme activity in early succession following forest fire. Forests 8:347.

Kolka, R., B. Sturtevant, P. Townsend, J. Miesel, P. Wolter, S. Fraver, and T. DeSutter. 2014. Post-fire comparisons of forest floor and soil carbon, nitrogen, and mercury pools with fire severity indices. Soil Science Society of America Journal 78: S58–S65.

Kurth, V. J., N. Fransioli, P. Z. Fulé, S. C. Hart, and C. A. Gehring. 2013. Stand-replacing wildfires alter the community structure of wood-inhabiting fungi in southwestern ponderosa pine forests of the USA. Fungal Ecology 6:192–204.

Kurth, V. J., S. C. Hart, C. S. Ross, J. P. Kaye, and P. Z. Fulé. 2014. Stand-replacing wildfires increase nitrification for decades in southwestern ponderosa pine forests. Oecologia 175:395–407.

Lau, J. A., and J. T. Lennon. 2012. Rapid responses of soil microorganisms improve plant fitness in novel environments. Proceedings of the National Academy of Sciences USA 109:201202319.

Lennon, J. T., and S. E. Jones. 2011. Microbial seed banks: the ecological and evolutionary implications of dormancy. Nature Reviews Microbiology 9:119–130.

Leprince, F., and H. Quiquampoix. 1996. Extracellular enzyme activity in soil: effect of pH and ionic strength on the interaction with montmorillonite of two acid phosphatases secreted by the ectomycorrhizal fungus *Hebeloma cylindrosporum*. European Journal of Soil Science 47:511–522.

Levin, S. A. 1992. The problem of pattern and scale in ecology: the Robert H. MacArthur Award Lecture. Ecology 73:1943–1967.

Long, X.-E., C. Chen, Z. Xu, and J. He. 2014. Shifts in the abundance and community structure of soil ammonia oxidizers in a wet sclerophyll forest under long-term prescribed burning. Science of the Total Environment 470–471:578–586.

MacKenzie, M. D., T. H. DeLuca, and A. Sala. 2004. Forest structure and organic horizon analysis along a fire chronosequence in the low elevation forests of western Montana. Forest Ecology and Management 203:331–343.

Mallek, C., H. Safford, J. Viers, and J. Miller. 2013. Modern departures in fire severity and area vary by forest type, Sierra Nevada and southern Cascades, California, USA. Ecosphere 4:1–28.

McGinnis, T. W., J. E. Keeley, S. L. Stephens, and G. B. Roller. 2010. Fuel buildup and potential fire behavior after stand-replacing fires, logging fire-killed trees and herbicide shrub removal in Sierra Nevada forests. Forest Ecology and Management 260:22–35.

Miesel, J. R., R. E. J. Boerner, and C. N. Skinner. 2011. Soil nitrogen mineralization and enzymatic activities in fire and fire surrogate treatments in California. Canadian Journal of Soil Science 91:935–946.

Miesel, J., A. Reiner, C. Ewell, B. Maestrini, and M. Dickinson. 2018. Quantifying changes in total and pyrogenic carbon stocks across fire severity gradients using active wildfire incidents. Frontiers in Earth Science 6:1.

Miller, J. D., and H. D. Safford. 2017. Corroborating evidence of a pre-Euro-American low- to moderate-severity fire regime in yellow pine-mixed conifer forests of the Sierra Nevada, California, USA. Fire Ecology 13:58–90.

Miller, J. D., and A. E. Thode. 2007. Quantifying burn severity in a heterogeneous landscape with a relative version of the delta Normalized Burn Ratio (dNBR). Remote Sensing of Environment 109:66–80.

Miller, J. D., E. E. Knapp, C. H. Key, C. N. Skinner, C. J. Isbell, R. M. Creasy, and J. W. Sherlock. 2009*a*. Calibration and validation of the relative differenced Normalized Burn Ratio (RdNBR) to three measures of fire severity in the Sierra Nevada and Klamath Mountains, California, USA. Remote Sensing of Environment 113:645–656.

Miller, J. D., H. D. Safford, M. Crimmins, and A. E. Thode. 2009*b*. Quantitative evidence for increasing forest fire severity in the Sierra Nevada and Southern Cascade Mountains, California and Nevada, USA. Ecosystems 12:16–32.

Nave, L. E., E. D. Vance, C. W. Swanston, and P. S. Curtis. 2011. Fire effects on temperate forest soil C and N storage. Ecological Applications 21:1189–1201.

Neary, D. G., C. C. Klopatek, L. F. DeBano, and P. F. Folliott. 1999. Fire effects on belowground sustainability: a review and synthesis. Forest Ecology and Management 122:51–71.

Parker, K. W. 1951. A method for measuring trend in range condition on national forest ranges. Forest Service, U.S. Department of Agriculture, Washington, D.C., USA.

Pellegrini, A. F. A., et al. 2018. Fire frequency drives decadal changes in soil carbon and nitrogen and ecosystem productivity. Nature 553:194.

Pickett, S. T. A. 1989. Space-for-time substitution as an alternative to long-term studies. Pages 110–135 *in* G. E. Likens, editor. Long-term studies in ecology. Springer, New York, New York, USA.

Qi, Y., and M. Xu. 2001. Separating the effects of moisture and temperature on soil CO2 efflux in a coniferous forest in the Sierra Nevada mountains. Plant and Soil 237:15–23.

R Development Core Team. 2008. R: a language and environment for statistical computing. R Foundation for Statistical Computing, Vienna, Australia. www.R-project.org

Restaino, C. R., and H. D. Safford. 2018. Fire and climate change. Pages 493505 in J. W. van Wagtendonk, N. G. Sugihara, S. L. Stephens, A. E. Thode, K. E. Shaffer, and J. A. Fites-Kaufman, editors. Fire in Californias ecosystems, 2nd edition. University of California Press, Berkeley, California, USA.

Robinson, N. P., B. W. Allred, M. O. Jones, A. Moreno, J. S. Kimball, D. E. Naugle, T. A. Erickson, and A. D. Richardson. 2017. A dynamic Landsat derived normalized difference vegetation index (NDVI) product for the conterminous United States. Remote Sensing 9:863.

Ross, C. S., J. P. Kaye, M. W. Kaye, V. J. Kurth, R. Brimmer, S. C. Hart, and P. Z. Fulé. 2012. Ecosystem carbon remains low for three decades following fire and constrains soil CO_2 responses to precipitation in southwestern ponderosa pine forests. Ecosystems 15:725–740.

Rousk, J., and S. D. Frey. 2015. Revisiting the hypothesis that fungal-to-bacterial dominance characterizes turnover of soil organic matter and nutrients. Ecological Monographs 85:457–472.

Ryu, S.-R., A. Concilio, J. Chen, M. North, and S. Ma. 2009. Prescribed burning and mechanical thinning effects on belowground conditions and soil respiration in a mixed-conifer forest, California. Forest Ecology and Management 257:1324–1332.

Saetre, P. 1999. Spatial patterns of ground vegetation, soil microbial biomass and activity in a mixed spruce-birch stand. Ecography 22:183–192.

Safford, H. D., and J. T. Stevens. 2017. Natural Range of Variation (NRV) for yellow pine and mixed conifer forests in the Sierra Nevada, southern Cascades, and Modoc and Inyo National Forests, California, USA. General Technical Report PSW-GTR-256. USDA Forest Service Pacific Southwest Research Station, Albany, CA, USA.

Safford, H. D., and K. M. van de Water. 2014. Using fire return interval departure (FRID) analysis to map spatial and temporal changes in fire frequency on national forest. Research Paper. USDA Forest Service Pacific Southwest Research Station, Albany, CA, USA.

Safford, H. D., J. D. Miller, D. A. Schmidt, B. Roath, and A. Parsons. 2008. BAER soil burn severity maps do not measure fire effects to vegetation: a comment on Odion and Hanson (2006). Ecosystems 11:1–11.

Safford, H. D., D. A. Schmidt, and C. H. Carlson. 2009. Effects of fuel treatments on fire severity in an area of wildland–urban interface, Angora Fire, Lake Tahoe Basin, California. Forest Ecology and Management 258:773–787.

Santos, F., M. S. Torn, and J. A. Bird. 2012. Biological degradation of pyrogenic organic matter in temperate forest soils. Soil Biology and Biochemistry 51:115–124.

Schimel, J., T. C. Balser, and M. Wallenstein. 2007. Microbial stress-response physiology and its implications for ecosystem function. Ecology 88:1386–1394.

Segers, R. 1998. Methane production and methane consumption: a review of processes underlying wetland methane fluxes. Biogeochemistry 41:23–51.

Sinsabaugh, R. L., et al. 2008. Stoichiometry of soil enzyme activity at global scale. Ecology Letters 11:1252–1264.

Smithwick, E. A. H., M. G. Turner, M. C. Mack, and F. S. Chapin. 2005. Postfire soil N cycling in Northern conifer forests affected by severe, stand-replacing wildfires. Ecosystems 8:163–181.

St. John, T. V., and P. W. Rundel. 1976. The role of fire as a mineralizing agent in a Sierran coniferous forest. Oecologia 25:35–45.

Stark, J. M., and M. K. Firestone. 1995. Mechanisms for soil moisture effects on activity of nitrifying bacteria. Applied and Environmental Microbiology 61:218–221.

Stark, J. M., and S. C. Hart. 1997. High rates of nitrification and nitrate turnover in undisturbed coniferous forests. Nature 385:61–64.

Steel, Z. L., M. J. Koontz, and H. D. Safford. 2018. The changing landscape of wildfire: burn pattern trends and implications for California's yellow pine and mixed conifer forests. Landscape Ecology 33:1159–1176.

Stenberg, B., M. Johansson, M. Pell, K. Sjödahl-Svensson, J. Stenström, and L. Torstensson. 1998. Microbial biomass and activities in soil as affected by frozen and cold storage. Soil Biology and Biochemistry 30:393–402.

Stephens, S. L., et al. 2014. Temperate and boreal forest megafires: characteristics and challenges. Frontiers in Ecology and the Environment 12:115–122.

Sullivan, B. W., T. E. Kolb, S. C. Hart, J. P. Kaye, B. A. Hungate, S. Dore, and M. Montes-Helu. 2011. Wildfire reduces carbon dioxide efflux and increases methane uptake in ponderosa pine forest soils of the southwestern USA. Biogeochemistry 104:251–265.

Sun, H., M. Santalahti, J. Pumpanen, K. Köster, F. Berninger, T. Raffaello, F. O. Asiegbu, and J. Heinonsalo. 2016. Bacterial community structure and function shift across a northern boreal forest fire chronosequence. Scientific Reports 6:1–12.

Taş, N., E. Prestat, J. W. McFarland, K. P. Wickland, R. Knight, A. A. Berhe, T. Jorgenson, M. P. Waldrop, and J. K. Jansson. 2014. Impact of fire on active layer and permafrost microbial communities and metagenomes in an upland Alaskan boreal forest. ISME Journal 8:1904–1919.

Turner, B. L. 2010. Variation in pH optima of hydrolytic enzyme activities in tropical rain forest soils. Applied and Environmental Microbiology 76:6485–6493.

Turner, M. G., E. A. H. Smithwick, K. L. Metzger, D. B. Tinker, and W. H. Romme. 2007. Inorganic nitrogen availability after severe stand-replacing fire in the Greater Yellowstone ecosystem. Proceedings of the National Academy of Sciences USA 104:4782–4789.

USDA-NRCS. 2015. Soil Survey Geographic (SSURGO) Database for California. https://www.nrcs.usda.gov/wps/portal/nrcs/detail/soils/survey/?cid=nrcs142p2_053627

Vance, E. D., P. C. Brookes, and D. S. Jenkinson. 1987. An extraction method for measuring soil microbial biomass C. Soil Biology and Biochemistry 19:703–707.

Wang, Y., Z. Xu, and Q. Zhou. 2014. Impact of fire on soil gross nitrogen transformations in forest ecosystems. Journal of Soils and Sediments 14:1030–1040.

Westerling, A. L., H. G. Hidalgo, D. R. Cayan, and T. W. Swetnam. 2006. Warming and earlier spring increase Western U.S. Forest Wildfire Activity. Science 313:940–943.

Whitman, T., C. Pepe-Ranney, A. Enders, C. Koechli, A. Campbell, D. H. Buckley, and J. Lehmann. 2016. Dynamics of microbial community composition and soil organic carbon mineralization in soil following addition of pyrogenic and fresh organic matter. ISME Journal 10:2918–2930.

Yeager, C. M., D. E. Northup, C. C. Grow, S. M. Barns, and C. R. Kuske. 2005. Changes in nitrogen-fixing and ammonia-oxidizing bacterial communities in soil of a mixed conifer forest after wildfire. Applied and Environmental Microbiology 71:2713–2722.

Zibilske, L. M. 1994. Carbon mineralization. Pages 835–863 In Methods of Soil Analysis: Part 2—Microbiological and Biochemical Properties sssabookseries. Soil Science Society of America, Madison, Wisconsin, USA.

SUPPORTING INFORMATION

Additional supporting information may be found online at: http://onlinelibrary.wiley.com/doi/10.1002/eap.2072/full

DATA AVAILABILITY

Data are available from the Dryad Digital Repository: https://doi.org/10.6071/m3c09w.